Springer

KSME

Journal of Mechanical Science and Technology 26 (12) (2012) 3795~3801
www.springerlink.com/content/1738-494x
DOI 10.1007/s12206-012-1006-2

On the dynamics of capillary imbibition †

Jungchul Kim and Ho-Young Kim*

School of Mechanical and Aerospace Engineering, Seoul National University, Seoul, 151-744, Korea

(Manuscript Received May 15, 2012; Revised July 9, 2012; Accepted July 23, 2012)

Abstract

The imbibition of wetting liquids in porous media takes place on length scales spanning several orders of magnitude, in phenomena ranging from landslide due to heavy rainfall in geophysics to stiction of nanopatterns in semiconductor manufacturing. We review the current theoretical understanding of the dynamics of liquid infiltration that are driven by capillary forces and resisted by viscous friction. Physical principles that govern the flows in smooth channels and porous media, either with or without gravitational effects, are explained with simplified mathematical solutions. Also, some important but unexplored topics associated with capillary imbibition are suggested.

Keywords: Wetting; Surface tension; Porous media; Drops

1. Introduction

When a liquid drop is brought into contact with a wettable solid surface, it spontaneously spreads over the surface. It is the capillary force that drives the flow to minimize the free energy of the solid-liquid-gas system [1]. Wettable solids are energetically more stable when wet than dry. The same physical principle is at work for wettable narrow channels or porous media contacting liquids. They imbibe liquids by capillary action. Natural and industrial processes associated with capillary impregnation abound, including ink on paper, dye in fabric, oil in a porous rock, water in soil, sap in xylem or a biofluid in cartilage. Capillary phenomena also play an important role in various fields of nano- and bio-technology. Nanoscale patterns on semiconductor wafers may stick together due to the surface tension of an evaporating rinsing solution [2, 3], which is one of the major problems deteriorating production yield. Many lab-on-a-chip systems rely on capillary forces to pump liquid into channels [4, 5].

From a fluid-dynamic point of view, the wicking flows are often laminar and slow, the analysis for which can be considered classical if the effects of the liquid front, or contact line, can be neglected. Major difficulties of understanding the dynamics of wicking come from the incomplete knowledge of formation and motion of three-phase (solid-liquid-fluid) contact lines. Furthermore, the inherently complex geometry of pore structures in most porous media aggravates theoretical understanding and experimental measurements of wicking flows. As a result, a number of unanswered capillary-imbibition problems remain, which occur in various fields of science and engineering.

In the following, we review the current understanding of the capillary imbibition dynamics by classifying the flows by the character of solid (or fluid conduit): flows in smooth channels and porous media. In Section 2, we introduce governing equations for capillary flows in smooth channels and explain various characters of the flows when the channels are horizontal and vertical. Flows wicking into porous media are treated in Section 3, where the basic analysis tools and important flow characteristics are introduced. We conclude by suggesting some mundane but practically important problems that wait for theoretical explanations and experimental measurements.

2. Capillary flows in smooth channels

2.1 Governing equations and boundary conditions

In most cases, inertial effects in capillary flows are negligibly small compared to other effects due to capillarity and viscosity. This does not necessarily imply that the Reynolds number of the flow is much smaller than unity. Even when the Reynolds number is not small, the thinness of fluid conduits often allows us to neglect inertia, or to use the *lubrication approximation* [6, 7]. For a flow in a capillary with a radius a and an axial length L, one can show that the flow velocity, u, is dominantly in the axial direction (x) and only varies in radial direction (r) provided that $a/L \ll 1$ and $(a/L)^2 \,\mathrm{Re} \ll 1$, where the Reynolds number is defined as $\mathrm{Re} = \rho U a/\mu$ with ρ and μ being the density and the viscosity of the liquid, re-

*Corresponding author. Tel.: +82 2 880 9286, Fax.: +82 2 880 9287
E-mail address: hyk@snu.ac.kr
† This paper was presented at the Workshop honoring professor Jung Yul Yoo on his Official Retirement, Seoul, Korea, March 2012.

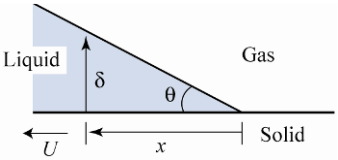

Fig. 1. Schematic of a liquid wedge and moving contact line. The solid is shown to move with a relative velocity U to the stationary liquid-gas interface.

spectively, and U the average velocity. Also, it follows that the pressure, p, is a function of the axial direction, x, and time (if unsteady), t, only. Then the governing equation becomes, in cylindrical coordinates,

$$\frac{\partial p(x,t)}{\partial x} = \mu \frac{1}{r} \frac{\partial}{\partial r}\left[r \frac{\partial u(r,t)}{\partial r} \right]. \tag{1}$$

The radius a may be allowed to vary slowly with either t or x while still using Eq. (1) because the one-dimensional, fully-developed character of the flow still holds. When Re is much smaller than unity, we need not resort to the lubrication approximation in order to neglect inertia forces - the Stokes equation can be formally used:

$$\nabla p = \mu \nabla^2 u \ . \tag{2}$$

The velocity of liquid at a solid wall follows that of the solid in general, which is referred to as the no-slip boundary condition. In microscale channel flows, however, the liquid has been observed to slip, or move with nonzero relative velocity, at the solid boundary when the solid is nonwettable and the shear rate is high [8-10]. Such a slip boundary condition may be considered irrelevant to wicking, which usually involves wettable solids. However, one needs to be cautious when applying the no-slip boundary condition at the moving contact line. Consider a contact line moving with a steady velocity U, or equivalently, a stationary contact line located on a substrate moving with a steady velocity U, as shown in Fig. 1. Here, we assume that the contact angle, θ, is small so that the lubrication equation can be used. The shear stress at the solid wall can be scaled as $\tau_s \sim \mu U / \delta$, where δ is the height of the liquid-gas interface which can be approximated as $\delta \approx x\theta$. Throughout this paper, θ denotes the contact angle either static or dynamic; the contact angle alone is a very rich topic, whose detailed discussion is beyond the scope of this work [11, 12]. The viscous shear force per unit depth, F, near the contact line is obtained by integrating τ from $x = 0$ to Λ, where Λ is the characteristic extension of the wedge:

$$F \sim \mu \int_0^{\Lambda} \frac{U}{x\theta} dx \ . \tag{3}$$

This integration is logarithmically singular at $x = 0$. A similar logarithmic singularity of the shear force occurs when the contact angle is large as well [13-15]. This is the famous *contact line singularity*, which inevitably occurs when the no-slip boundary condition is applied at the contact line. The singularity is only relieved when the contact angle becomes 180º [16]. This mathematical singularity can be circumvented based on various physical arguments [11], including the statistical motion of fluid molecules [17], a diffuse interface model [18], etc. More conveniently, the integration can be cut off at a small distance λ from the contact line, which is argued to be of the order of molecular size [11, 14]. Then we get $F \sim (\mu U / \theta) \ln(\Lambda / \lambda)$ for either small or large value of the contact angle. The exact value of Λ / λ is not very important because its logarithmic value is used [15].

The shape of the liquid-fluid interface is determined by the kinematic and dynamic boundary conditions. When the equation of the interface is written as $\xi(x, y, z, t) = 0$, the kinematic boundary condition, which is based on mass conservation, is written as [19]

$$\frac{d\xi}{dx} = 0 \ . \tag{4}$$

The force balance at the interface yields the dynamic boundary conditions (DBC), which can be written in normal and tangential directions respectively as [6]

$$p_2 - p_1 + \sigma\kappa = 2\mu_2 \frac{\partial u_{n,2}}{\partial n} - 2\mu_1 \frac{\partial u_{n,1}}{\partial n}, \tag{5}$$

$$\mu_2 \left(\frac{\partial u_{n,2}}{\partial \tau} + \frac{\partial u_{\tau,2}}{\partial n} \right) - \mu_1 \left(\frac{\partial u_{n,1}}{\partial \tau} + \frac{\partial u_{\tau,1}}{\partial n} \right) = \frac{\partial \sigma}{\partial \tau}, \tag{6}$$

where σ is the surface tension, κ is the curvature of the interface, n and τ denote the normal and tangential directions, respectively. Subscripts 1 and 2 denote the fluids separated by the interface. The normal DBC, Eq. (5), signifies that a jump in normal stress occurs across the interface, which is equal to the Laplace pressure, $\sigma\kappa$. When the right-hand side of Eq. (5) is neglected, we recover the Young-Laplace equation: $p_1 - p_2 = \sigma\kappa$ [22, 23]. The tangential DBC, Eq. (6), states that discontinuity in the shear stress at the interface arises when the surface tension gradient exists in the tangential direction. This is a basic mechanism leading to the Marangoni flows [20].

2.2 Dynamics of imbibition into horizontal channels

Consider a horizontal channel connected to a liquid reservoir on one side and exposed to the atmosphere on the other, as shown in Fig. 2(a). We are interested in predicting the capillary imbibition velocity as a function of the liquid properties and channel geometry. The flow is driven by the pressure difference between the liquid front and the reservoir, $p_1 - p_a$, and resisted by the viscous stress. For a circular channel, Eq. (1) can be analytically solved to give the average imbibition

velocity $U = Q/A$, where Q is the volume flow rate and A is the cross-sectional area of the channel. However, for channels with noncircular cross-sectional shapes, e.g., polygons or ellipses, using the Darcy friction factor, f_D, provides a more convenient path to obtain U. Here, f_D is defined as

$$f_D = \left(-\frac{dp}{dx} \right) \frac{2D_h}{\rho U^2} \tag{7}$$

with D_h being the hydraulic diameter. For fully-developed flows, we can write $f_D Re = C$, where the value of a constant C is known for various geometries [21]. For a circular channel with a radius a and a contact angle θ, $-dp/dx = 2\sigma\cos\theta/(ax)$, $D_h = 2a$, and $C = 64$. Hence, we get $U = -dx/dt = \sigma a\cos\theta/(8\mu x)$. Solving for x as a function of t leads to the so-called Washburn equation [24], stating that x diffusively increases with time:

$$x = (Dt)^{1/2} \tag{8}$$

where the effective diffusivity $D = \frac{1}{4}\sigma a\cos\theta/\mu$. Recently, Reyssat et al. [25] pointed out that Bell and Cameron [26] and Lucas [27] had found the result even before Washburn.

In the following, we introduce an alternative approach that is more suited for deriving a scaling law of the wetting velocity on rough, as well as smooth, surfaces. For a smooth horizontal channel, the surface free energy of the liquid-solid system decreases with the capillary imbibition. As the liquid front propagates into the channel of the hydraulic diameter D_h by dx, the surface energy changes by $dE = -\pi D_h(\sigma_{SG} - \sigma_{SL})dx$, where σ_{SG} and σ_{SL} are the solid-gas and solid-liquid interfacial energy per unit area, respectively. The driving force F_d is then given by $F_d = -dE/dx = \pi D_h\sigma\cos\theta$, where we used Young's equation [22], $\sigma_{LG}\cos\theta = \sigma_{SG} - \sigma_{SL}$, where the liquid-gas interfacial energy per unit area $\sigma_{LG} = \sigma$. The resisting force due to viscous shear stress, τ_s, is scaled as $F_r = \int_0^x 2\pi\mu U dx$, where we have assumed that the dissipation in the region far from the contact line dominates over the dissipation at the contact line [15]. For flows with negligible inertia, the driving and resisting forces are balanced, $F_d \sim F_r$, leading to the scaling relation of a capillary imbibition velocity, $U = D_h\sigma\cos\theta/(\mu x)$.

2.3 Dynamics of capillary rise in vertical tubes

Now we consider a channel situated along the gravitational direction as shown in Fig. 2(b). When the interior wall of the channel is wettable, the liquid rises against gravity, a phenomenon called *capillary rise*. The equilibrium height at which the height of the liquid column, ρgV, with g being the gravitational acceleration and V the column volume, is balanced by the upward surface tension force, $\pi D_h\sigma\cos\theta$, is referred to as Jurin's height after a British scientist who first

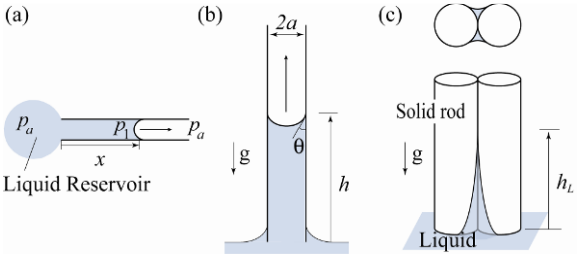

Fig. 2. (a) Capillary imbibition into a horizontal channel; (b) Capillary rise in a vertical tube; (c) Capillary rise in a corner.

observed this functional dependency in the early eighteenth century [28]. For a circular tube, Jurin's height reads $h_J = 2\sigma\cos\theta/(\rho ga)$. The rate of the capillary rise can be obtained in a similar manner to ones for the foregoing horizontal imbibition but with $-dp/dx = (\sigma\kappa - \rho gh)/h$, where h is the rise height. For a circular tube in which the velocity profile at any instant of time is assumed to be given by the Poiseuille profile, the equation of motion becomes [29]

$$\frac{\mu}{\sigma}\frac{dh}{dt} = \frac{1}{8}\left(\frac{2a\cos\theta}{h} - \frac{\rho ga^2}{\sigma} \right). \tag{9}$$

Integration gives the relationship between the rise time and height:

$$t = T\left(\ln\frac{1}{1 - h/h_J} - \frac{h}{h_J} \right) \tag{10}$$

where $T = 8\mu h_J/(\rho ga^2)$. For short times when $h/h_J \ll 1$, Eq. (10) is reduced to the Washburn equation.

While the foregoing model assumes a fully developed velocity profile, in the very early stages of capillary rise of liquid with a very low viscosity, the flow is resisted by inertia rather than viscous friction. It was shown that the liquid rises linearly with time in this regime, with the speed scaled as $c \sim [\sigma/(\rho a)]^{1/2}$ [30].

Unlike the capillary rise within a tube of a finite cross-sectional area, the liquid in a sharp corner formed by two solid cylinders, as shown in Fig. 2(c), can rise without limit theoretically since the radius of the meniscus curvature can reach zero [31]. The flow is still driven by capillarity and resisted by gravity and viscosity. Thus, the following scaling relation based on the Stokes equation can be written:

$$\frac{\mu}{rh} \sim \rho g + \mu\frac{U}{r^2} \tag{11}$$

where r is the characteristic radius of meniscus which changes with h. The radius of leading meniscus r_L decreases as the liquid rises:

$$r_L = \left(\frac{\mu\sigma}{\rho^2 g^2 t} \right)^{1/3}. \tag{12}$$

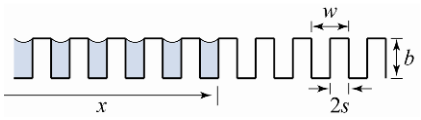

Fig. 3. Hemi-wicking within porous surface.

For small r_L, gravitational effects can be neglected and Eqs. (11) and (12) yield a scaling law for the height of capillary rise in a corner [31]:

$$h_L = \left(\frac{\sigma^2 t}{\mu \rho g} \right)^{1/3} . \tag{13}$$

It is remarkable that the capillary rise in a corner follows a power law ($t^{1/3}$) different from Washburn's law ($t^{1/2}$).

3. Imbibition into porous media

3.1 Horizontal flow

The physics behind wicking into porous media is not fundamentally different from that of capillary imbibition into a smooth channel - capillary forces drive and viscous friction resists the flow, whose balance determines the flow velocity. A major difficulty in understanding the flow into porous media arises due to the complex internal geometry of the media; size, structure, tortuosity and wetted portion of pores that are hard to measure precisely. Such a problem is somewhat relieved when the flow occurs over a porous, or rough, surface whose structure can be quantified easily compared to the pores within a bulk. When a liquid contacts a highly wettable surface with sub-millimetric roughness, the surface is impregnated with the liquid, as shown in Fig. 3. This process is referred to as *hemi-wicking* [32] since it corresponds to wicking on a two-dimensional surface, not wicking into three-dimensional space.

The decrease of the interfacial energy as a liquid front advances by dx is given by

$$dE = -(f - \phi_t)(\sigma_{SG} - \sigma_{SG})dx + (1 - \phi_t)\sigma dx \tag{14}$$

where f is the roughness defined as the ratio of the actual surface area to the projected area and ϕ_t is the area fraction of the surface that remains dry. For a square pillar array as shown in Fig. 3, with cylinders of radius s, height b, and pitch w, the roughness f is given by $f = 1 + \pi sb / w^2$. The driving force is given by $F_d = -dE/dx = (f-1)\sigma$ when the contact angle is nearly zero. $F_d = 0$ for a smooth surface ($f = 1$). This implies that hemi-wicking occurs only on rough surfaces - a different approach should be employed to analyze the *spreading* on smooth surfaces [11, 33], which is beyond the scope of the current review. The friction on the rough surface arises from the liquid viscosity. When the protrusions (of a characteristic height b) are short compared to the pitch (w) between them, i.e., $b < w$, the dominant friction is due to velocity gradients over a distance b. Then the resisting force is given by $F_r \sim \mu Ux/b$. On the other hand, when $b \gg w$, the friction predominantly takes place against the protrusions [34]. For cylindrical pillar arrays with a pillar radius s, $F_r \sim \mu Ubx / [w^2 \ln(w/s)]$. Srivastava et al. [35] derived scaling laws applicable to wide range of geometric factors, such as pillar size and pitch, using finite element simulations. As long as F_r is proportional to x, which is the case in hemi-wicking, balancing F_d and F_r yields the Washburn equation: $x \propto t^{1/2}$. The axisymmetric hemi-wicking, which occurs as a fluid-filled pen gently touches a micropillar array, also exhibits the diffusive behavior: $R \propto t^{1/2}$, where R is the radius of the circular wet area [36].

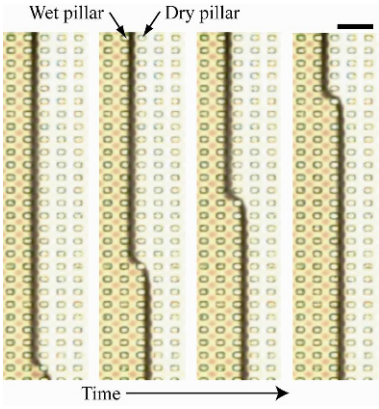

Fig. 4. Image sequence of zippering wet front. The liquid is water and the substrate is a superhydrophilic square array of silicon square micropillars with 25, 10 and 10 μm in pitch, height and side length, respectively. Scale bar, 50 μm.

Recently, it was found that the wet front can propagate over a rough surface in two qualitatively different modes, depending on the strength of liquid source (either a spreading drop or a tube that supplies liquid toward the edge). When a drop is deposited on a rough surface (e.g., a micropillar array), it initially spreads to develop a circular fringe layer while the central bulk collapses. The radial extension of the thin film surrounding the bulk shows diffusive behavior. However, in the late stages when the bulk is almost diminished, the fringe layer advances through faceted zippering as shown in Fig. 4. By zippering, we refer to the motion of a liquid front through which a dry row of pillars facing the existing wet row of pillars is wetted as if the wet front were zipped. The wet area expands in a direction perpendicular to the rows going through consecutive zippering. This causes the final footprint to be polygonal, revealing the lattice structure of the micropillars [37]. The faceted zippering of a wet front can be also realized using a fluid-filled pen. If the pen is pressed so that no gap is present between the pen tip and the top of surface protrusions, the leakage of the bulk flow is prevented. Then the liquid may wet only through the spacing between the pillars. Such a zippering front propagates under a power law ($t^{1/3}$) different from the Washburn equation [38]. When the bulk leaks from the tip,

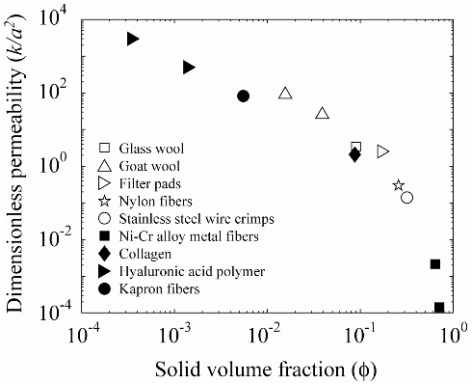

Fig. 5. Permeability of various fibrous media as a function of the solid volume fraction [42].

which is usually the case unless the conformal contact as described above is achieved, the spreading front propagates axisymmetrically, obeying the Washburn law.

As a liquid infiltrates into a bulk medium with complex pore network, simple hydrodynamic models as above are not applicable. It is known that the liquid velocity is proportional to the pressure gradient and inversely proportional to the viscosity [39, 40]:

$$u = -\frac{k}{\mu}\nabla p \tag{15}$$

where k is the permeability. This equation, referred to as Darcy's law, is widely used in engineering applications especially for Newtonian fluids at low flow rates [41]. The permeability k depends on the size, concentration and arrangement of pore structures [42]. For fibrous porous media, e.g., fabrics and paper, k is a function of fiber radius (a), volume fraction of solid material (ϕ) and the fiber arrangement [42]:

$$\frac{k}{a^2} = f(\phi)\,. \tag{16}$$

Fig. 5 shows the experimentally measured permeability of various fibrous media [42]. If x is the distance from the source to the edge of the wetting front, the velocity $u \sim dx/dt$. Provided that the capillary pressure that drives the flow is kept constant, which is usually the case when the pore size ($\sim \kappa^{-1}$) is uniform throughout the medium, we get $|\nabla p| \sim \sigma\kappa/x$ [43]. Then we can recover the Washburn equation, $x \sim (k\sigma\kappa/\mu)^{1/2}t^{1/2}$, from Eq. (15).

3.2 Vertical flow

As in the previous section, we start with the rise of a liquid through hemi-wicking along a vertically situated rough surface. In early times, the dynamics are governed by capillarity and viscous resistance while gravity can be neglected [34]. Thus, the rise rate follows the Washburn law. Xiao et al. [44] obtained accurate values of the effective diffusivity D in Eq. (8) for micropillar arrays through simulations and experiments. In late times when the gravitational effects become significant, the rise rate greatly deviates from that of the Washburn equation. In addition to the hydrostatic effects, the liquid film thickness, which affects both the capillary pressure and viscous shear stress, can change as a function of the height. This is a topic worthy of further exploration.

For a liquid infiltrating into a bulk porous medium against gravity, a modified form of Darcy's law is used:

$$u = -\frac{k}{\mu}(-\nabla p + \rho g)\,. \tag{17}$$

If the liquid within the rigid porous medium is incompressible, we write $\nabla \cdot u = 0$. Then Eq. (17) gives $\nabla^2 p = 0$. Solving this Laplace equation with suitable boundary conditions for p can completely specify the flow via Eq. (17) [43]. For large enough times, the Washburn equation is known to fail to match experimental measurements in some types of porous media [45, 46]. Attempts have been made to explain power laws that are different from the Washburn equation in late times [46, 47]. Delker et al. [45] modeled the capillary rise dynamics in porous media as a metastable stick-slip behavior, and experimentally found that $u \sim t^{-3/4}$ in a packed bead structure, which gives the rise height $h \sim t^{1/4}$. In late times, pores are not necessarily filled completely with liquid because of significantly weakened driving forces. This may be an important reason why the rise rate does not obey the Washburn dynamics, although this possibility has not been theoretically explored yet.

4. Conclusions

We have reviewed the current understanding of the dynamics of capillary imbibition into various types of solid structures. Although fundamental equations and solution methods have been established for many cases just as many other branches in fluid dynamics, still there are many important yet unexplored phenomena in this area. We conclude with briefly listing these exciting novel problems awaiting mathematical modeling and quantitative experiments. First, with the rapid development of micro- and nano-scale fabrication technology, many thin structures are used as liquid channels. Because thin structures are inherently flexible, capillary flows in the channel can develop forces (by surface tension σ and capillary pressure $\sigma\kappa$) strong enough to deform the channel [48-50]. The deformation of channel geometry alters the driving and resisting forces, which eventually modifies the capillary imbibition rate [51, 52]. Second, besides thin-walled channels, many porous media found in natural and industrial situations, such as soil [53], paper [54], biological tissues [55] and food [56], are deformable. The interaction of deformable porous media with pressurized fluid flows has been intensively stud-

ied since Biot [57], but one with flows driven by capillary forces has attracted little attention so far: in particular, cellulose fiber networks, such as sponges [47] and paper, swell and soften as absorbing moisture. Then the pore size and tortuosity, and eventually, the capillary imbibition rate are altered. To one's surprise, no theoretical tools exist to understand such ubiquitous phenomena. Lastly, chemical potential as well as mechanical pressure participates in liquid transport in some porous media, such as plant xylem and hydrogel. In general, the ability to absorb water increases as the solute concentration increases, which plant cells utilize to control the water transport rate [58]. Investigating this process can help us to understand how water can climb up in a tree as tall as 100 m without a mechanical pump [59] (meaning that water molecules are under tension at 10 m or higher from the ground). Also, this study will allow us to control the deformation of hydrogels [60], which find a variety of applications in biomedical technology [61].

Acknowledgment

This work was supported by National Research Foundation of Korea (Grant Nos. 2009-008284, 2011-0030744, and 2012-008023) and administered by SNU-IAMD.

References

[1] A. W. Adamson and A. P. Gast, *Physical Chemistry of Surfaces*, Sixth Ed. Wiley, New York, USA (1997).

[2] C. H. Mastrangelo and C. H. Hsu, Mechanical stability and adhesion of microstructures under capillary forces - Part I: Basic theory, *J. Microelectromech. Syst. 2* (1993) 33-43.

[3] N. Chakrapani, B. Wei, A. Carrillo, P. M. Ajaya and R. S. Kane, Capillarity-driven assembly of two-dimensional cellular carbon nanotube foams, *Proc. Nat. Acad. Sci.* USA 101 (2004) 4009-4012.

[4] M. Zimmermann, H. Schmid, P. Hunziker and E. Delamarche, *Capillary pumps for autonomous capillary systems, Lab Chip 7* (2007) 119-125.

[5] H. Cho, H.-Y. Kim, J. Y. Kang and T. S. Kim, How the capillary burst microvalve works, *J. Colloid Interface Sci*. 306 (2007) 379-385.

[6] G. K. Batchelor, *An Introduction to Fluid Dynamics*, Cambridge Univ. Press, Cambridge, UK (1967).

[7] A. Oron, S. H. Davis and S. G. Bankoff, Long-scale evolution of thin liquid films, *Rev. Mod. Phys*. 69 (1997) 931-980.

[8] D. C. Tretheway and C. D. Meinhart, Apparent fluid slip at hydrophobic microchannel walls, *Phys. Fluids* 14 (2002) L9-L12.

[9] M. Majumder, N. Chopra, R. Andrews and B. J. Hinds, Enhanced flows in carbon nanotubes, *Nature* 438 (2005) 44.

[10] P. Huang, J. S. Guasto and K. S. Breuer, Direct measurement of slip velocities using three-dimensional total internal reflection velocimetry, *J. Fluid Mech*. 566 (2006) 447-464.

[11] P. G. de Gennes, Wetting: statics and dynamics, *Rev. Mod. Phys*. 50 (1985) 827-863.

[12] P. G. de Gennes, F. Brochard-Wyart and D. Quéré, *Capillarity and Wetting Phenomena: Drops, Bubbles, Pearls, Waves*, Springer, New York, USA (2004).

[13] C. Huh and L. E. Scriven, Hydrodynamic model of steady movement of a solid/liquid/fluid contact line, *J. Colloid Interface Sci*. 35 (1971) 85-101.

[14] H. -Y. Kim, H. J. Lee and B. H. Kang, Sliding of liquid drops down an inclined solid surface, *J. Colloid Interface Sci*. 247 (2002) 372-380.

[15] H. -Y. Kim, On thermocapillary propulsion of microliquid slug, *Nanoscale Microscale Thermophys. Eng*. 11 (2007) 351-362.

[16] L. Mahadevan and Y. Pomeau, Rolling droplets, Phys. Fluids 11 (1999) 2449-2453.

[17] T. D. Blake and J. M. Haynes, Kinetics of liquid/liquid displacement, *J. Colloid Interface Sci*. 30 (1969) 421-423.

[18] P. Yue, C. Zhou and J. J. Feng, Sharp-interface limit of Cahn-Hilliard model for moving contact lines, *J. Fluid Mech*. 645 (2010), 279-294.

[19] H. Lamb, *Hydrodynamics*, Sixth Ed. Cambridge Univ. Press, Cambridge, UK (1932).

[20] L. E. Scriven and C. V. Sternling, The Marangoni effect, *Nature* 187 (1960) 186-188.

[21] K. V. Sharp, R. J. Adrian, J. G. Santiago and J. I. Molho, Liquid flows in microchannels, in *The MEMS Handbook*, M. Gad-el-Hak (ed), CRC Press, Boca Raton, Florida, USA (2002).

[22] T. Young, An essay on the cohesion of fluids, *Phil. Trans. Roy. Soc. London* 95 (1805) 65-87.

[23] P. S. Laplace, Mecanique *Celeste* Supplement to the 10th edition, Courier, Paris (1806).

[24] E. W. Washburn, The dynamics of capillary flow, *Phys. Rev*. 17 (1921) 273-283.

[25] M. Reyssat, L. Courbin, E. Reyssat and H. A. Stone, Imbibition in geometries with axia variations, *J. Fluid Mech*. 615 (2008) 335-344.

[26] J. M. Bell and F. K. Cameron, The flow of liquids through capillary spaces, *J. Phys. Chem*. 10 (1906) 658-674.

[27] V. R. Lucas, Ueber das zeitgesetz des kapillaren aufstiegs von flüssigkeiten. *Kolloid Zeistschrift* 23 (1918) 15-22.

[28] J. Jurin, An account of some experiments shown before the Royal Society; With an enquiry into the cause of the ascent and suspension of water in capillary tubes, *Phil. Trans*. 30 (1717-1719) 739-747.

[29] R. F. Probstein, *Physicochemical Hydrodynamics: An Introduction* second ed., Wiley, New York, USA (1994).

[30] D. Quéré, Inertial capillarity, *Europhys. Lett*. 39 (1997) 533-538.

[31] A. Ponomarenko, D. Quéré and C. Clanet, A universal law for capillary rise in corners, *J. Fluid Mech*. 666 (2011) 146-154.

[32] J. Bico, C. Tordeux and D. Quéré, Wetting of textured surfaces, *Europhys. Lett*. 55 (2002) 214-220.

[33] D. Bonn, J. Eggers, J. Indekeu, J. Meunier and E. Rolley,

Wetting and spreading, *Rev. Mod. Phys*. 81 (2009) 739-805.
[34] C. Ishino, M. Reyssat, E. Reyssat, K. Okumura and D. Quéré, Wicking within forests of micropillars, *Europhys. Lett*. 79 (2007) 56005.
[35] N. Srivastava, C. Din, A. Judson, N. C. MacDonald and C. D. A. Meinhart, Unified scaling model for flow through a lattice of microfabricated posts, *Lab Chip* 10 (2010) 1148-1152.
[36] J. Kim, M.-W. Moon, K. -R. Lee, L. Mahadevan and H. -Y. Kim, Hydrodynamics of writing with ink, *Phys. Rev. Lett*. 107 (2011) 264501.
[37] L. Courbin, E. Denieul, E. Dressaire, M. Roper, A. Ajdari and H. A. Stone, Imbibition by polygonal spreading on microdecorated surfaces, *Nature Mat*. 6 (2007) 661-664.
[38] S. J. Kim, M. -W. Moon, K. -R. Lee, D. -Y. Lee, Y. S. Chang and H. -Y. Kim, Liquid spreading on superhydrophilic miropillar arrays, *J. Fluid Mech*. 680 (2011) 477-487.
[39] H. Darcy, Les Fontaines de la *Ville de Dijon*, Victor Dalmont, Paris (1856).
[40] H. F. Wang, Theory of Linear Poroelasticity with Applications to Geomechanics and Hydrogeology, Princeton Univ. Press, Princeton, New Jersey, USA (2000).
[41] M. Landeryou, I. Eames and A. Cottenden, Infiltration into inclined fibrous sheets, *J. Fluid Mech*. 529 (2005) 173-193.
[42] G. W. Jackson and D. F. James, The permeability of fibrous porous media, Can. *J. Chem. Eng*. 64 (1986) 364-374.
[43] D. Vella and H. E. Huppert, The waterlogging of floating objects, J. Fluid Mech. 585 (2007) 245-254.
[44] R. Xiao, R. Enright and E. N. Wang, Prediction of liquid propagation in micropillar arrays, *Langmuir* 26 (2010) 15070-15075.
[45] T. Delker, D. B. Pengra and P. -Z. Wong, Interface pinning and dynamics of capillary rise in porous media, *Phys. Rev. Lett*. 76 (1996) 2902-2905.
[46] M. Lago and M. Araujo, Capillary rise in porous media, *J. Colloid Interface Sci*. 234 (2001) 35-43.
[47] J. I. Siddique, D. M. Anderson and A. Bondarev, Capillary rise of a liquid into a deformable porous material, *Phys. Fluids* 21 (2009) 013106.
[48] J. Bico, B. Roman, L. Moulin and A. Boudaoud, Elastocapillary coalescence in wet hair, *Nature* 432 (2004) 690.
[49] H.-Y. Kim and L. Mahadevan, Capillary rise between elastic sheets, *J. Fluid Mech*. 548 (2006) 141-150.
[50] J. W. van Honschoten, E. Escalante, N. R. Tas, H. V. Jansen and M. Elwenspoek, Elastocapillary filling of deformable nanochannels, *J. Appl. Phys*. 101 (2007) 094310.
[51] J. M. Aristoff, C. Duprat and H. A. Stone, Elastocapillary imbibition, Int. *J. Nonlin. Mech*. 46 (2011) 648-656.
[52] C. Duprat, J. M. Aristoff and H. A. Stone, Dynamics of elastocapillary rise, *J. Fluid Mech*. 679 (2011) 641-654.
[53] J. Bear, Dynamics of Fluids in Porous *Media*, Dover, New York (1972).
[54] E. Reyssat and L. Mahadevan, How wet paper curls, *Europhys. Lett*. 93 (2011) 54001.
[55] J. M. Skotheim and L. Mahadevan, Dynamics of poroelastic filaments, *Proc. Roy. Soc. London A*, 460 (2004) 1995-2020.
[56] L. Fisher, Physics takes the biscuit, *Nature* 397 (1999) 469.
[57] M. A. Biot, General theory of three-dimensional consolidation, *J. Appl. Phys*. 12 (1941) 155- 165.
[58] L. Taiz and E. Zeiger, *Plant Physiology*, Fifth Ed. Sinauer Associates, Sunderland, Massachusetts, USA (2010).
[59] T. D. Wheeler and A. D. Strook, The transpiration of water at negative pressures in a synthetic tree, *Nature* 455 (2008) 208-212.
[60] J. Yoon, S. Cai, Z. Suo and R. C. Hayward, Poroelastic swelling kinetics of thin hydrogel layers: comparison of theory and experiment, *Soft Matter* 6 (2010) 6004-6012.
[61] N. A. Peppas, Y. Huang, M. Torres-Lugo, J. H. Ward and J. Zhang, Physicochemical foundations and structural design of hydrogels in medicine and biology, *Ann. Rev. Biomed. Eng*. 2 (2000) 9-29.

Jungchul Kim received a B.S. degree from POSTECH in Mechanical Engineering, in 2009. He is currently a Ph.D candidate at the School of Mechanical and Aerospace Engineering in Seoul National University. His research interests are in capillary-driven flows and poro-elasto capillarity.

Ho-Young Kim received his B.S. degree from Seoul National University and S.M. and Ph.D degrees from MIT all in Mechanical Engineering. He is now an associate professor of mechanical engineering at Seoul National University. His research activities revolve around classical physics with particular interests in capillary-driven flows, poro-elasto-capillarity and biolocomotion.